

# **Transfer Relation between the Compression Test Rig and the Anthropomorphic Test Device (ATD) Lower Leg**

**by Masayuki Sakamoto**

**ARL-SR-0330**

**August 2015**

## **NOTICES**

### **Disclaimers**

The findings in this report are not to be construed as an official Department of the Army position unless so designated by other authorized documents.

Citation of manufacturer's or trade names does not constitute an official endorsement or approval of the use thereof.

Destroy this report when it is no longer needed. Do not return it to the originator.

# **Army Research Laboratory**

Adelphi, MD 20783-1138

---

**ARL-SR-0330****August 2015**

---

## **Transfer Relation between the Compression Test Rig and the Anthropomorphic Test Device (ATD) Lower Leg**

**Masayuki Sakamoto**

**Japanese ESEP Research Engineer**

**at Weapons and Materials Research Directorate, ARL**

REPORT DOCUMENTATION PAGE				Form Approved OMB No. 0704-0188	
<p>Public reporting burden for this collection of information is estimated to average 1 hour per response, including the time for reviewing instructions, searching existing data sources, gathering and maintaining the data needed, and completing and reviewing the collection information. Send comments regarding this burden estimate or any other aspect of this collection of information, including suggestions for reducing the burden, to Department of Defense, Washington Headquarters Services, Directorate for Information Operations and Reports (0704-0188), 1215 Jefferson Davis Highway, Suite 1204, Arlington, VA 22202-4302. Respondents should be aware that notwithstanding any other provision of law, no person shall be subject to any penalty for failing to comply with a collection of information if it does not display a currently valid OMB control number.</p> <p><b>PLEASE DO NOT RETURN YOUR FORM TO THE ABOVE ADDRESS.</b></p>					
1. REPORT DATE (DD-MM-YYYY) August 2015		2. REPORT TYPE ESEP activity		3. DATES COVERED (From - To) 04/2014–09/2014	
4. TITLE AND SUBTITLE Transfer Relation between the Compression Test Rig and the Anthropomorphic Test Device (ATD) Lower Leg				5a. CONTRACT NUMBER	
				5b. GRANT NUMBER	
				5c. PROGRAM ELEMENT NUMBER	
6. AUTHOR(S) Masayuki Sakamoto (Japanese Engineer Scientist Exchange Program Research Engineer)				5d. PROJECT NUMBER ESEP	
				5e. TASK NUMBER	
				5f. WORK UNIT NUMBER	
7. PERFORMING ORGANIZATION NAME(S) AND ADDRESS(ES) US Army Research Laboratory ATTN: RDRL-WMP-F 2800 Powder Mill Road Adelphi, MD 20783-1138				8. PERFORMING ORGANIZATION REPORT NUMBER  ARL-SR-0330	
9. SPONSORING/MONITORING AGENCY NAME(S) AND ADDRESS(ES) Survivability and Firepower Analysis Section, Ballistic Research Division, Ground Systems Research Center ATTN: Masayuki Sakamoto 2-9-54, Fuchinobe, Chuo-ku, Sagamihara-shi, Kanagawa-ken 252-0206, JAPAN				10. SPONSOR/MONITOR'S ACRONYM(S)	
				11. SPONSOR/MONITOR'S REPORT NUMBER(S)	
12. DISTRIBUTION/AVAILABILITY STATEMENT Approved for public release; distribution unlimited.					
13. SUPPLEMENTARY NOTES Because one of the authors of this report is an employee of the Japanese Ministry of Defense (JMOD), this report cannot be published without approval by the appropriate Japanese organization. At the completion of the formal review process, and before publication, please forward this report to the Technical Research and Development Institute (TRDI), JMOD for approval to publish this report (JMOD/TRDI POC: Mr. Masayuki Sakamoto, Survivability and Firepower Analysis Section, Ballistic Research Division, Ground Systems Research Center [E-mail: <a href="mailto:masayuki@cs.trdi.mod.go.jp">masayuki@cs.trdi.mod.go.jp</a> , Phone:+81-42-752-2941, Address:2-9-54, Fuchinobe, Chuo-ku, Sagamihara-shi, Kanagawa-ken 252-0206, JAPAN]). Retain a copy of the approval with the Form-1 record.					
14. ABSTRACT This report was written by the author under the Engineer Scientist Exchange Program in the US Army Research Laboratory (ARL) from April 2013 to September 2014. We developed the Compression Test Rig (CTR) that is capable of evaluating the effectiveness of the blast-mitigating floor mat against assessed lower leg injury. The CTR was fabricated to simulate the loading status under the anthropomorphic test device (ATD) lower leg in the blast-loading event, and the transfer relation between the CTR response and ATD lower-leg response was clarified through the drop test with various loading conditions.					
15. SUBJECT TERMS ESEP, blast-mitigating floor mat, Evaluation methodology, Drop test					
16. SECURITY CLASSIFICATION OF:			17. LIMITATION OF ABSTRACT  UU	18. NUMBER OF PAGES  34	19a. NAME OF RESPONSIBLE PERSON Robert G Kargus
a. REPORT Unclassified	b. ABSTRACT Unclassified	c. THIS PAGE Unclassified			19b. TELEPHONE NUMBER (Include area code) (301) 394-5738

---

## Contents

---

<b>List of Figures</b>	<b>iv</b>
<b>List of Tables</b>	<b>v</b>
<b>Acknowledgments</b>	<b>vi</b>
<b>1. Introduction</b>	<b>1</b>
<b>2. Material and Methods</b>	<b>1</b>
2.1 Design of the CTR.....	1
2.2 Loading Test of the CTR and ATD Lower Leg .....	10
<b>3. Results and Discussion</b>	<b>13</b>
3.1 Experimental Results.....	13
3.2 Development of Transfer Relation .....	14
3.2 Prediction of ATD Lower-Leg Response Based on the CTR Response.....	20
<b>4. Conclusions</b>	<b>23</b>
<b>5. References</b>	<b>24</b>
<b>List of Symbols, Abbreviations, and Acronyms</b>	<b>25</b>
<b>Distribution List</b>	<b>26</b>

---

## List of Figures

---

Fig. 1	Conceptual drawing of the CTR.....	2
Fig. 2	Schematic of the response conversion between the CTR response and ATD lower-leg response.....	2
Fig. 3	FEA model for the ATD lower-leg loading.....	3
Fig. 4	Typical pressure distribution under the boot sole in the FEA result.....	4
Fig. 5	Load histories of the ATD lower leg in 10-meter-per-second (m/s), 10-millisecond (msec) pulse loading FEA.....	4
Fig. 6	FEA model for the CTR loading .....	5
Fig. 7	Load histories of the ATD lower leg and CTR (4.8 kg) in 10-m/s, 2.5-msec-pulse loading FEA.....	5
Fig. 8	Load histories of the ATD lower leg and CTR (4.8 kg) in 10-m/s, 5.0-msec-pulse loading FEA.....	6
Fig. 9	Load histories of the ATD lower leg and CTR (4.8 kg) in 10-m/s, 10-msec-pulse loading FEA.....	6
Fig. 10	Relation between the peak load and pulse duration .....	7
Fig. 11	Relation between the applied impulse and pulse duration.....	7
Fig. 12	Load histories of the ATD lower leg and CTR (1.3 kg) in 10-m/s, 2.5-msec-pulse loading FEA.....	8
Fig. 13	Load histories of the ATD lower leg and CTR (3.7 kg) in 10-m/s, 5-msec-pulse loading FEA.....	8
Fig. 14	Load histories of the ATD lower leg and CTR (6.6 kg) in 10-m/s, 10-msec-pulse loading FEA.....	9
Fig. 15	Drawings of the CTR prototype .....	10
Fig. 16	Arrangements of sensors in the test setup for the CTR loading .....	12
Fig. 17	Arrangements of sensors in the test setup for the ATD lower-leg loading.....	12
Fig. 18	Typical input- and output-acceleration histories in the CTR loading, CTR_03 (Height = 30 inches).....	13
Fig. 19	Typical input-acceleration history and ATD lower-tibia load history in the ATD lower-leg loading, ATD_03 (Height = 30 inches) .....	14
Fig. 20	Schematic of the transfer relation between the CTR response and ATD lower-leg response.....	15
Fig. 21	Synchronized crosshead-acceleration histories in the CTR loading .....	15
Fig. 22	Synchronized lower-tibia load histories in the ATD lower-leg loading .....	16
Fig. 23	Relation between the ATD lower-tibia load and CTR crosshead acceleration in	

each loading condition .....	16
Fig. 24 Schematic of the amplitude–domain transfer relation between the CTR response and ATD lower-leg response .....	17
Fig. 25 Relation between the duration and normalized response of the CTR loading .....	18
Fig. 26 Relation between the duration and normalized response in the ATD lower-leg loading .....	18
Fig. 27 Relation of the pulse duration between the ATD lower-tibia response and CTR crosshead response in each loading condition .....	19
Fig. 28 Schematic of the duration–domain transfer relation between the CTR response and ATD lower-leg response .....	20
Fig. 29 Comparison between the ATD lower-leg experimental response and predictive response from the CTR response, CTR_02/ATD_02 ( $\Delta V = 4.86$ m/s) .....	21
Fig. 30 Comparison between the ATD lower-leg experimental response and predictive response from the CTR response, CTR_04/ATD_04 ( $\Delta V = 6.26$ m/s) .....	21
Fig. 31 Example of the application of the transfer relation to the butyl-rubber floor mat in the FEA, CTR_03/ATD_03 ( $\Delta V = 5.26$ m/s) .....	22

---

## List of Tables

---

Table 1 FE material models for the floor-mat and floor-plate parts .....	3
Table 2 Specifications of the CTR .....	9
Table 3 Loading conditions for the CTR loading and ATD lower-leg loading .....	11
Table 4 Specifications of sensors used in the CTR loading and ATD lower-leg loading .....	13
Table 5 Average velocity changes in each loading condition .....	14
Table 6 Parameters for Eqs. 1 and 2 in each loading condition .....	17
Table 7 Parameters for Eq. 3 in each loading condition .....	20
Table 8 FE-material models for the butyl rubber .....	22
Table 9 Errors in the ATD lower-leg response prediction from the CTR response .....	23

---

## Acknowledgments

---

This report was written by the author under the Engineer Scientist Exchange Program in the US Army Research Laboratory (ARL) from April 2013 to September 2014. I would like to take this opportunity to thank the ARL for giving me the chance to learn and investigate blast-loading issues in the state-of-the-art research environment. I also would like to thank the members of the Blast Protection Branch and its specialists for supporting the numerical analysis, experiments, data processing, and various discussions that gave me valuable ideas. I especially appreciate ARL researcher Robert G Kargus's invitation for me to participate in the Underbody Blast Mitigation (UBM) program. This report was written in the collaborative research with him. Mr. Kargus invented the concept of the Compression Test Rig and energetically led its development and experimental verification. He also supported me in the writing and polishing of this report, for which I am sincerely grateful.

---

## 1. Introduction

---

Lower leg injury is a major injury mode induced by underbody blast loading associated with improvised explosive device (IED) attacks against ground fighting vehicles.<sup>1-4</sup> It is also widely believed that blast-mitigating floor mats are effective means for reducing the severity of lower leg injury.<sup>5-7</sup> Until now, it has been necessary to conduct the loading test with the anthropomorphic test device (ATD) lower leg for evaluations at the US Army Research Laboratory (ARL). However, the loading test with the ATD lower leg is expensive and time consuming; simplified methodology is in immediate need.

Under the auspices of the Underbody Blast Mitigation (UBM) program, we will develop the simplified methodology for the evaluation of floor-mat effectiveness. In this study, we developed the Compression Test Rig (CTR) that is capable of evaluating the mat's effectiveness against assessed lower leg injury. Firstly, we designed the CTR that represented the loading status under the ATD lower leg. Secondly, we conducted loading test of the nominal floor mat with the ATD lower leg and CTR. Then, we compared the responses to establish transfer relation between these 2 test configurations and investigated the applicability of the CTR in the floor-mat evaluation instead of the ATD lower leg.

---

## 2. Material and Methods

---

### 2.1 Design of the CTR

The CTR was designed as simple as possible to increase its availability to various stakeholders for the evaluation of the floor mat. The concept drawing of the CTR is shown in Fig. 1. In the testing, the CTR is fixed on the loading table of the drop tester, and the floor mat is compressed by the inertia of the indenter and crosshead; this produces an input and output relationship from the acceleration of the table and crosshead. In the evaluation, the crosshead acceleration is converted based on the transfer relation (Fig. 2) to the corresponding ATD lower-leg tibia load, which is a major criterion for the lower leg injury.

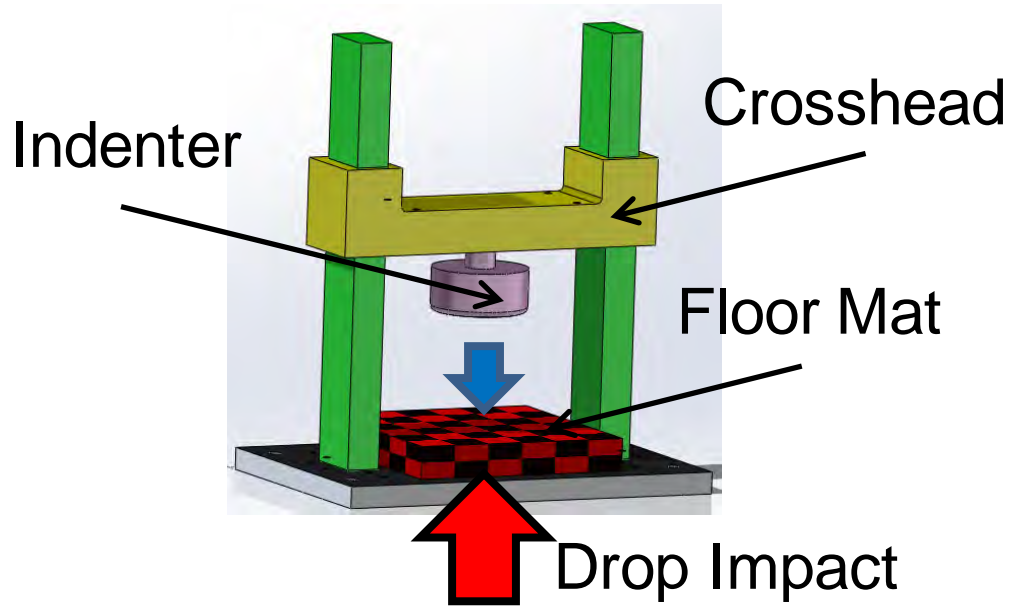


Fig. 1 Conceptual drawing of the CTR

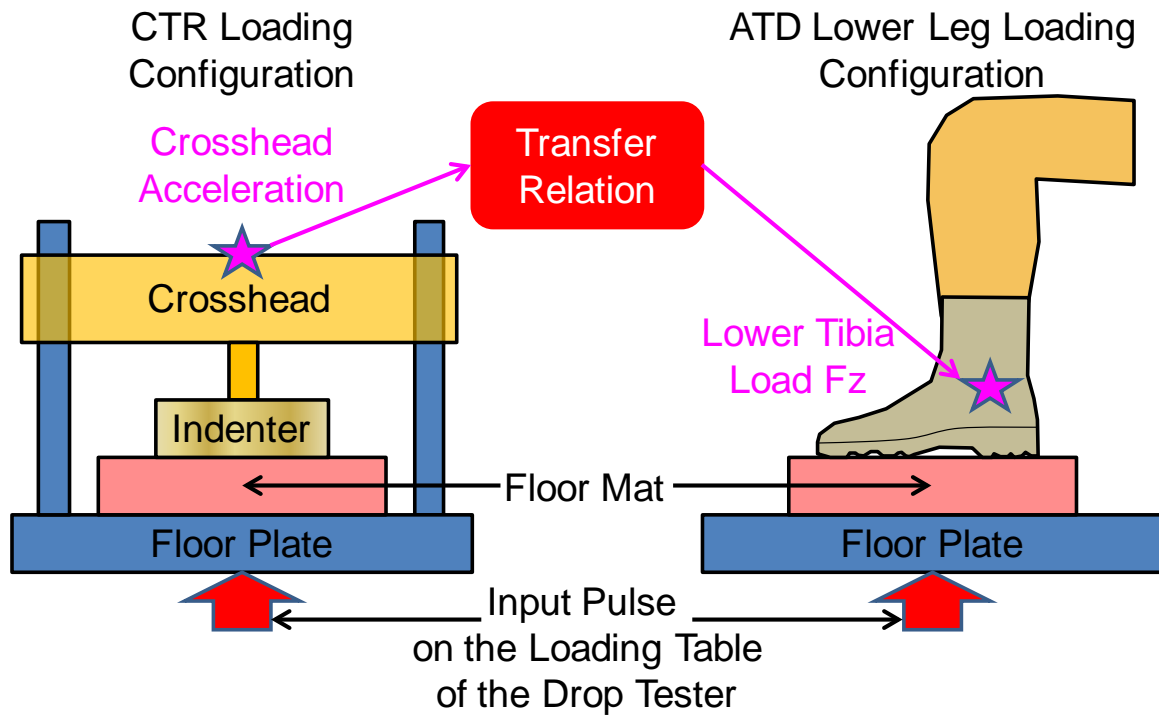
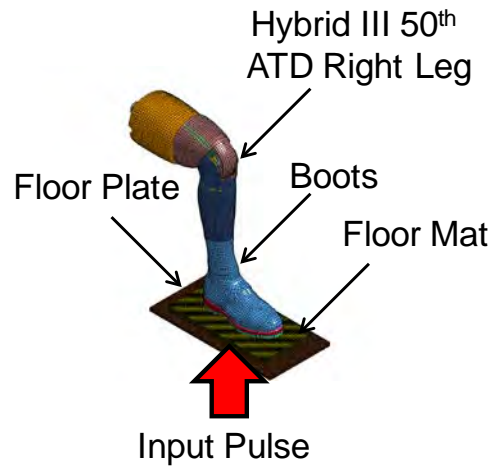


Fig. 2 Schematic of the response conversion between the CTR response and ATD lower-leg response

To simplify the transfer relation, it is necessary to generate the same material behavior in the floor mat between the CTR loading and ATD lower-leg loading. Therefore, we conducted the preliminary Finite Element Analysis (FEA) to clarify the loading status using the FE model of

the ATD lower-leg loading, as seen in Fig. 3. The FE-material models used in the floor-mat and floor-plate parts are listed in Table 1.



**Fig. 3 FEA model for the ATD lower-leg loading**

**Table 1 FE material models for the floor-mat and floor-plate parts**

Part	Material	Model Type in LS-DYNA	Model Description /Parameters
Floor Mat	Rubber	MAT_083_ FU_CHANG_FOAM	Form Type model with Strain Rate Dependent Hysteretic Unloading Behavior
Floor Plate	Aluminum	MAT_020_ RIGID	RO=2.816e-6 (kg/mm <sup>3</sup> ) E=70 (GPa) PR=0.30
CTR Indenter			

The pressure distribution under the boot sole was clarified (Fig. 4). There are high-pressure areas under the toe and heel. The load histories of a representative FEA result are shown in Fig. 5. Then, the tendency of loading by the boot heel and lower tibia is similar, although the boot toe shows different tendency. Therefore, it is convenient to generate similar loading status in the CTR loading as the boot-heel loading for the development of a simple transfer relation. Considering this, the cross-section of the CTR was determined to approximate the area of the boot heel. Moreover, the moving mass—indenter and crosshead—of the CTR was arranged temporarily as 4.8 kg (hereafter the fixed-mass CTR).

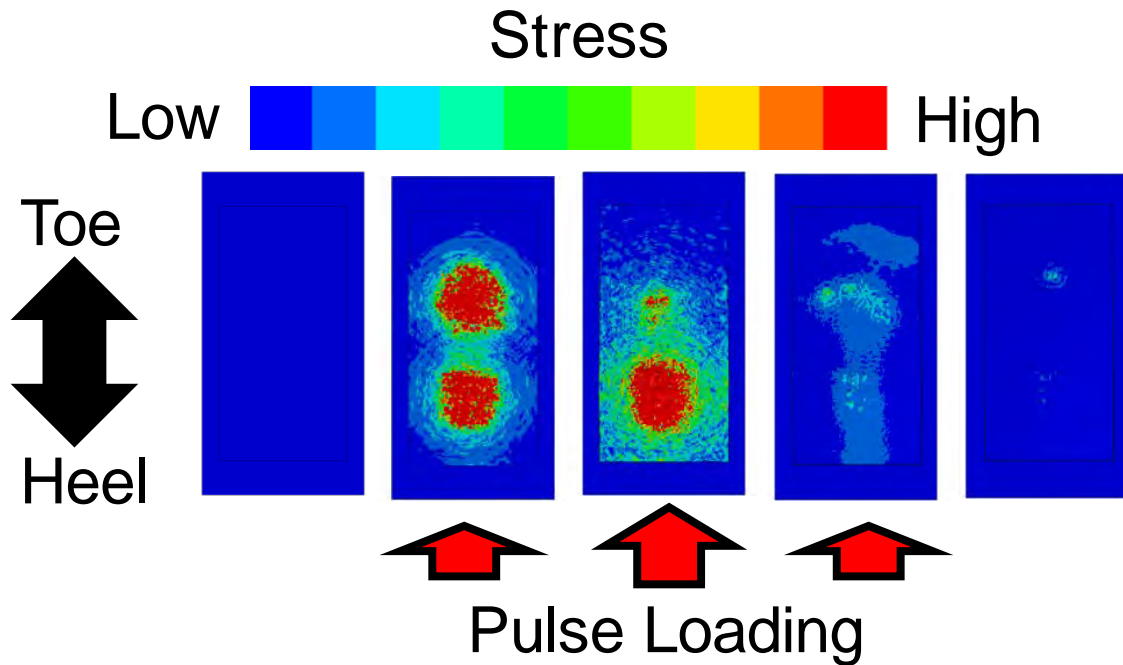


**Fig. 4** Typical pressure distribution under the boot sole in the FEA result

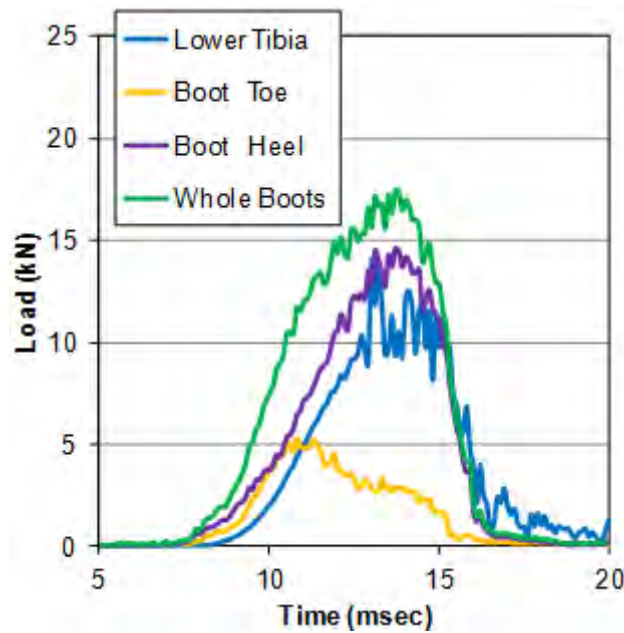


**Fig. 5** Load histories of the ATD lower leg in 10-meter-per-second (m/s), 10-millisecond (msec) pulse loading FEA

To confirm the loading status under this CTR indenter, FEAs were conducted in various loading conditions using the FE model, as illustrated in Fig. 6. The FE-material models used in this FE model were identical to those of the ATD lower-leg loading (Table 1).

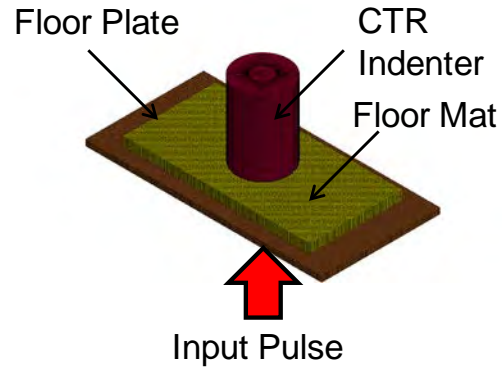


**Fig. 6 FEA model for the CTR loading**

The FEA results are shown in Figs. 7–9 with those of the ATD lower-leg loading. The loads applied by the CTR indenter differ from those applied by the boot heel.

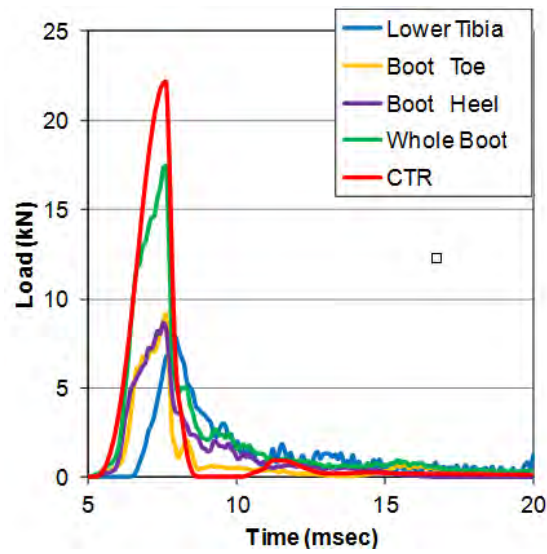


**Fig. 7 Load histories of the ATD lower leg and CTR (4.8 kg) in 10-m/s, 2.5-msec-pulse loading FEA**

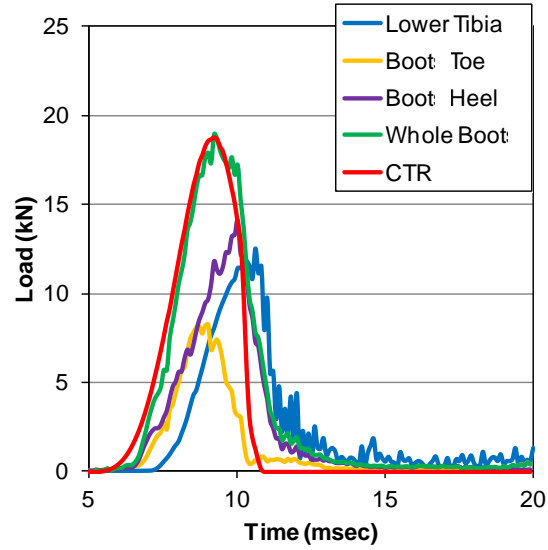


**Fig. 8 Load histories of the ATD lower leg and CTR (4.8 kg) in 10-m/s, 5.0-msec-pulse loading FEA**

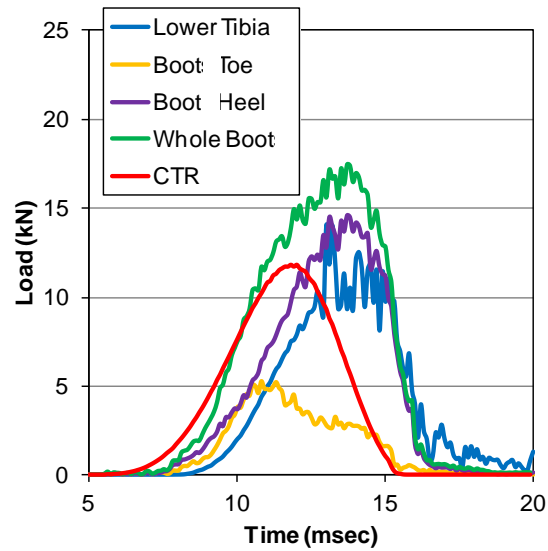


**Fig. 9 Load histories of the ATD lower leg and CTR (4.8 kg) in 10-m/s, 10-msec-pulse loading FEA**

To clarify this tendency, the peak loads and applied impulses are shown in Figs. 10 and 11. The fixed-mass CTR clearly shows a different loading tendency from the ATD lower leg, especially in the peak loads; thus we conclude that it is impossible to simulate the same loading condition as the boot heel with the fixed-mass CTR.

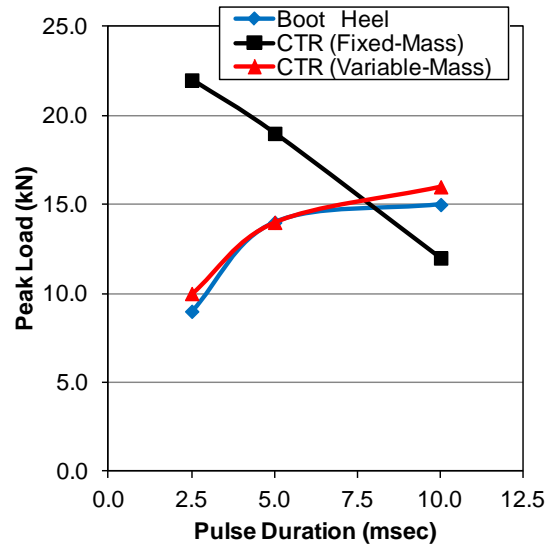


**Fig. 10 Relation between the peak load and pulse duration**

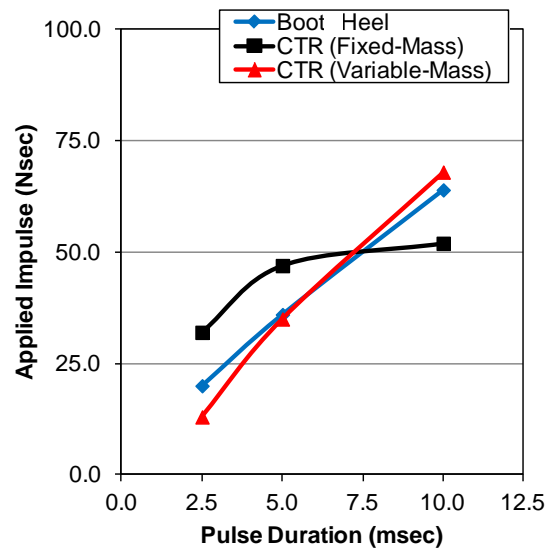


**Fig. 11 Relation between the applied impulse and pulse duration**

Additional analyses were conducted with CTRs that had various masses to determine the adequate mass for each loading pulse—hereafter, the variable-mass CTR—as shown in Figs. 12–14. (The FEA results are also summarized in Figs. 10 and 11.) Thus, there is agreement between the boot-heel loading and variable-mass CTR loading.

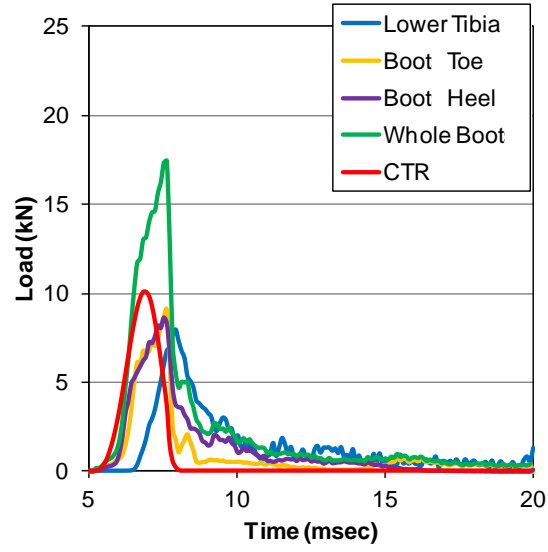


**Fig. 12 Load histories of the ATD lower leg and CTR (1.3 kg) in 10-m/s, 2.5-msec-pulse loading FEA**

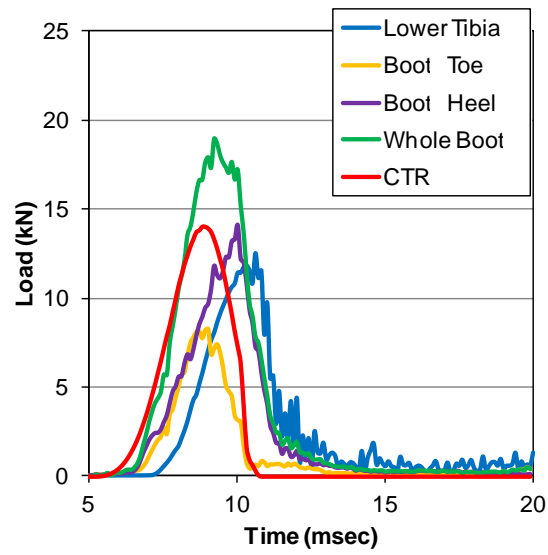


**Fig. 13 Load histories of the ATD lower leg and CTR (3.7 kg) in 10-m/s, 5-msec-pulse loading FEA**

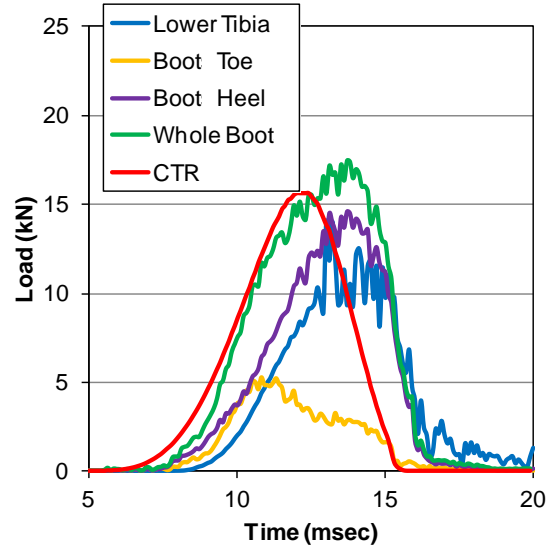


**Fig. 14 Load histories of the ATD lower leg and CTR (6.6 kg) in 10-m/s, 10-msec-pulse loading FEA**

In this study we focused on the 5-msec-pulse loading, which is one of the most frequent loading conditions in the evaluation of underbody blast loading. Therefore, the specifications of the CTR were determined (Table 2) by considering the relation between the CTR mass and response. According to these specifications, the CTR was fabricated as shown in Fig. 15.

**Table 2 Specifications of the CTR**

Specification	Target	Design
Moving Mass (Indenter+Crosshead) (kg)	3.7	3.9
Indenter Shape	-	Cylinder ( $\phi 4" \times 0.5"$ )
Indenter Cross-section (mm <sup>2</sup> )	9000	8200

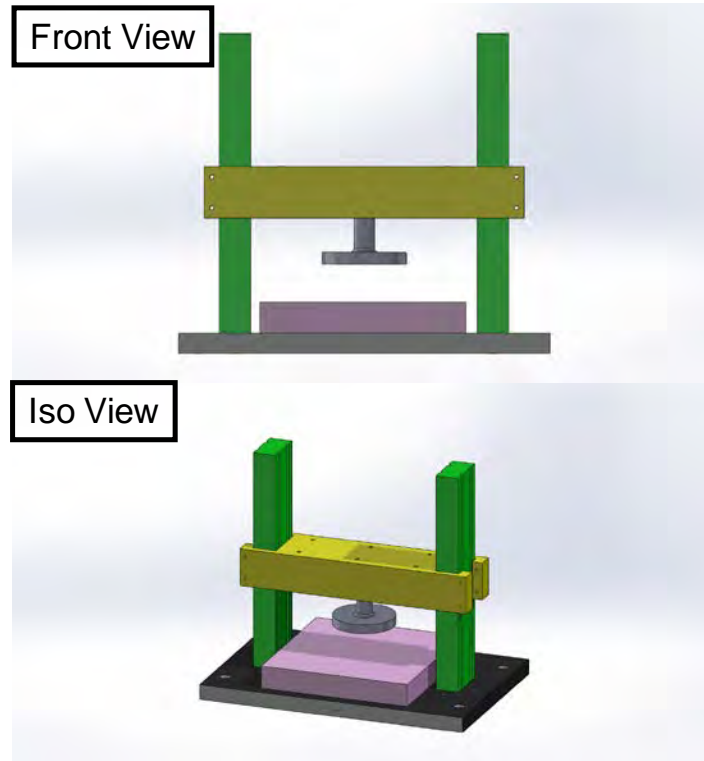


**Fig. 15 Drawings of the CTR prototype**

## **2.2 Loading Test of the CTR and ATD Lower Leg**

To develop the transfer relation between the CTR and ATD lower leg, the loading test with conditions in Table 3 were conducted in both test configurations. The responses of the CTR and ATD lower leg were measured in the crosshead acceleration and lower-tibia load, respectively. Moreover, SKYDEX material was used as the nominal floor mat in this loading test.

**Table 3 Loading conditions for the CTR loading and ATD lower-leg loading**

Test Apparatus	Pulse Duration, $\Delta T$ (msec)	Drop Height, H (inch)	Condition Code
CTR	5	15	CTR_01
		25	CTR_02
		30	CTR_03
		40	CTR_04
		45	CTR_05
ATD Lower Leg	5	15	ATD_01
		25	ATD_02
		30	ATD_03
		40	ATD_04
		45	ATD_05

The loading test was conducted on the drop testers (Lansmont, P65 and P45) at the Adelphi Laboratory Center, ARL. The arrangements of sensors in both test setups are shown in Figs. 16 and 17, and the specifications are listed in Table 4. The signals from sensors were recorded in the data-acquisition system (Spectral Dynamics, SYCHASVXI-5) at the sampling frequency of 250 kHz. Moreover, direct-current offset and the filters (Table 4) were applied to each signal in post-processing with the data-analysis software (MathWorks, MATLAB). The test was also recorded by the high-speed imaging camera (Phantom, Miro) for the confirmation of the test rig's behavior.

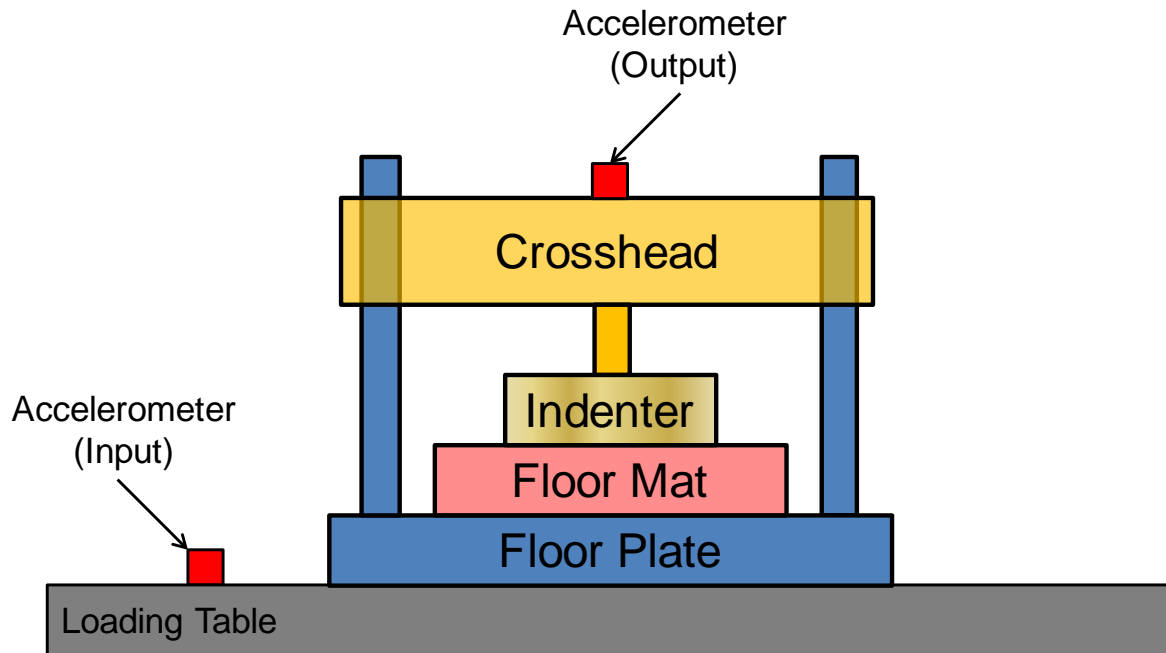


Fig. 16 Arrangements of sensors in the test setup for the CTR loading

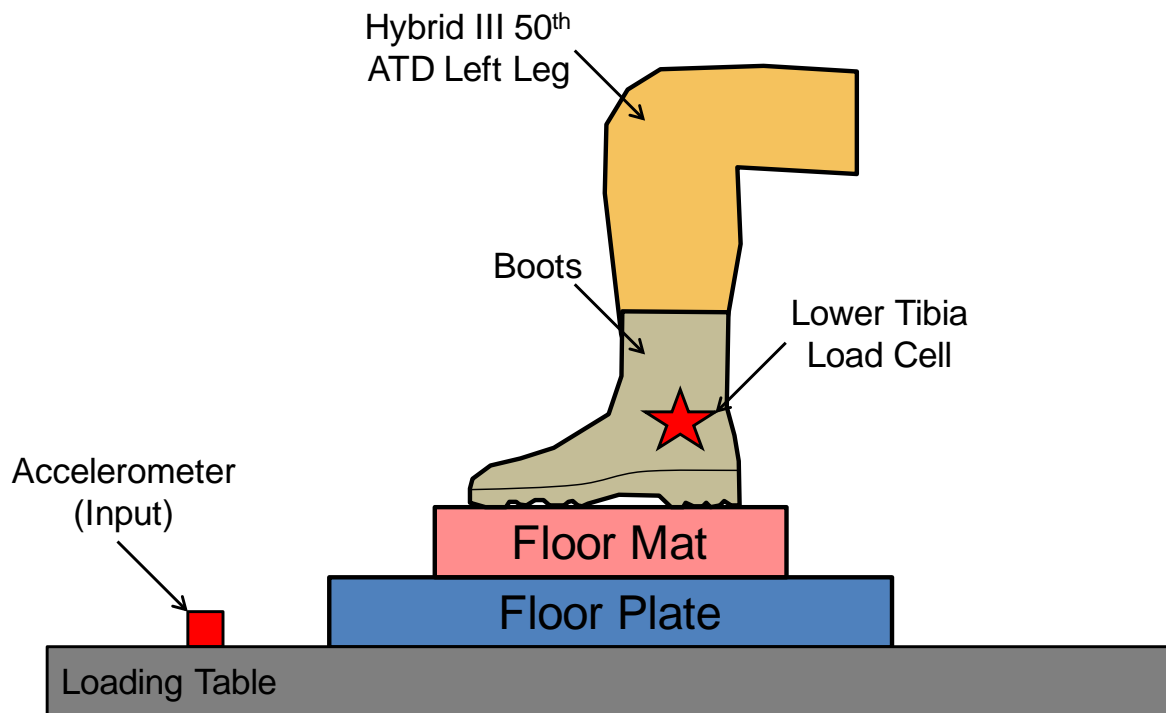


Fig. 17 Arrangements of sensors in the test setup for the ATD lower-leg loading

**Table 4** Specifications of sensors used in the CTR loading and ATD lower-leg loading

Sensor	Position	Type	Range	Filter
Load cell	ATD Lower Tibia	Denton 3644FL	10000lbf	CFC600
Acceleromete	Crosshead (Output)	Endevco 7270A-20KM6	20000G	CFC1000
Accelerometer	Loading Table (Input)	Endevco 7270A-60KM6	60000G	CFC1000

### 3. Results and Discussion

#### 3.1 Experimental Results

The typical responses of the CTR and ATD lower leg are shown in Figs. 18 and 19. The velocity change of each loading condition is summarized in Table 5. The responses show different delays in the peak value against the input pulses. Both responses have longer-duration pulses than their input-acceleration pulses, and the ATD lower leg shows longer-duration responses than the CTR. Moreover, there are plateau regions (second peaks) on the loading phase of the ATD lower-leg response, although the corresponding clues are not clear in the CTR response. These plateau regions were possibly generated as the results of the shock mitigation in the ATD foot flesh and boot sole and the floor mat.

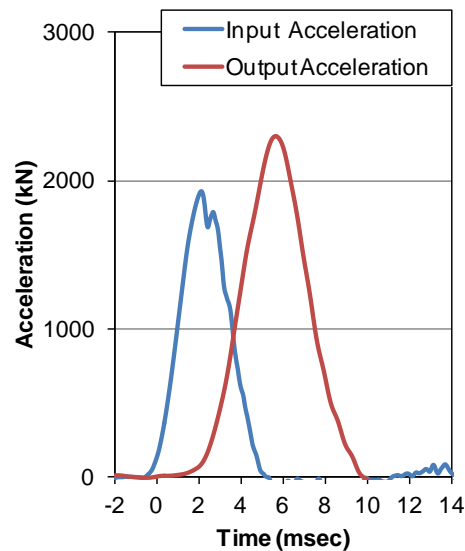


**Fig. 18** Typical input- and output-acceleration histories in the CTR loading, CTR\_03 (Height = 30 inches)

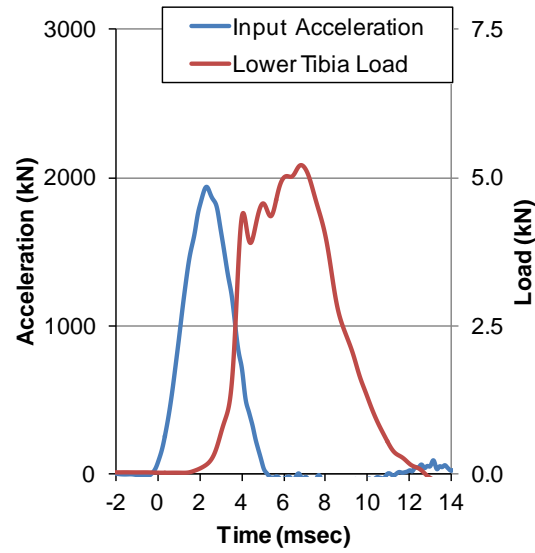


**Fig. 19 Typical input-acceleration history and ATD lower-tibia load history in the ATD lower-leg loading, ATD\_03 (Height = 30 inches)**

**Table 5 Average velocity changes in each loading condition**

Loading Condition	Drop Height, H (inch)	Velocity Change, $\Delta V(\text{m/s})$
CTR_01 / ATD_01	15	3.52
CTR_02 / ATD_02	25	4.86
CTR_03 / ATD_03	30	5.26
CTR_04 / ATD_04	40	6.26
CTR_05 / ATD_05	45	6.62

### 3.2 Development of Transfer Relation

The concept of the transfer relation developed in this study is shown in Fig. 20.<sup>8</sup> In this concept, the transfer relations were developed in the acceleration–force (amplitude–domain) transfer and time–time (duration–domain) transfer independently. To develop these transfer relations, it was necessary to compare the responses of the CTR and ATD lower leg in the amplitude domain and duration domain at each loading condition.

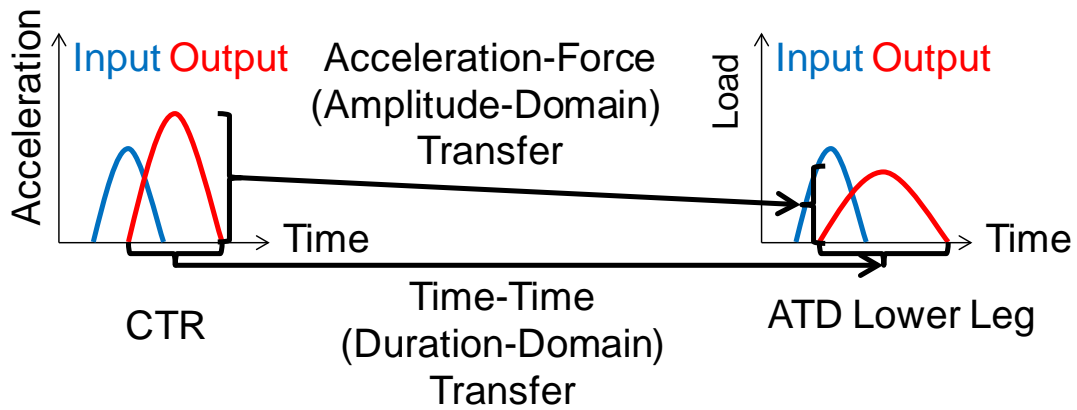


**Fig. 20** Schematic of the transfer relation between the CTR response and ATD lower-leg response

In the amplitude-domain comparison, the responses of the CTR and ATD lower leg were synchronized by setting their peaks to the time zero as shown in Figs. 21 and 22. Then, the responses of both test configurations were related in the amplitude domain as shown in Fig. 23.

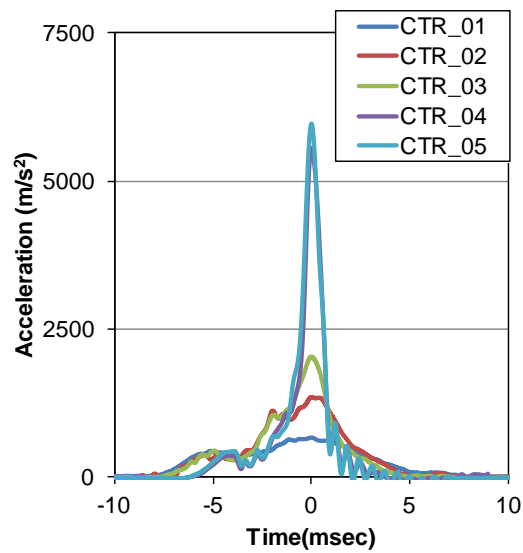


**Fig. 21** Synchronized crosshead-acceleration histories in the CTR loading

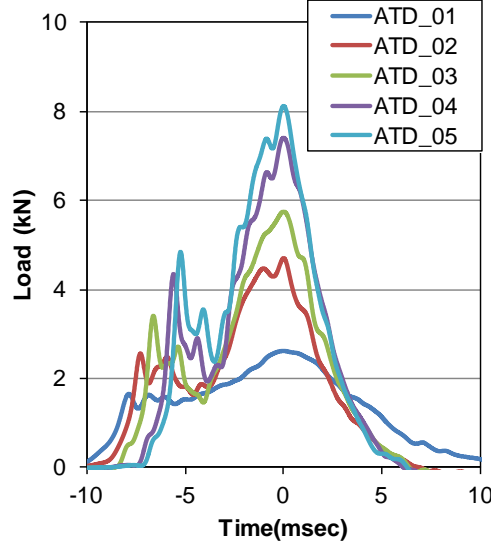


**Fig. 22 Synchronized lower-tibia load histories in the ATD lower-leg loading**

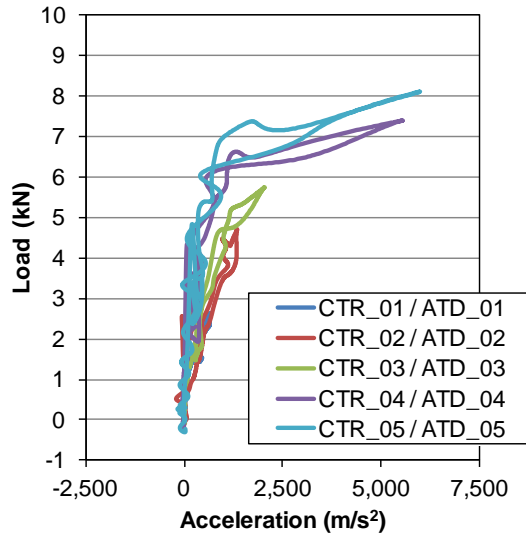


**Fig. 23 Relation between the ATD lower-tibia load and CTR crosshead acceleration in each loading condition**

There are 2 regions in the amplitude–domain transfer relation: nonlinear and linear (Fig. 24). Moreover, there is a rate effect in the slopes of the nonlinear region, whereas the slopes in the linear region are almost the same among test conditions and smaller than those of the nonlinear region. The smaller slopes in the linear regions are probably due to the plateau regions in the ATD lower-leg responses (shown in Fig. 22). The boundary between the nonlinear region and linear region was defined as the inflection point of the bilinear curve in the nonlinear region.

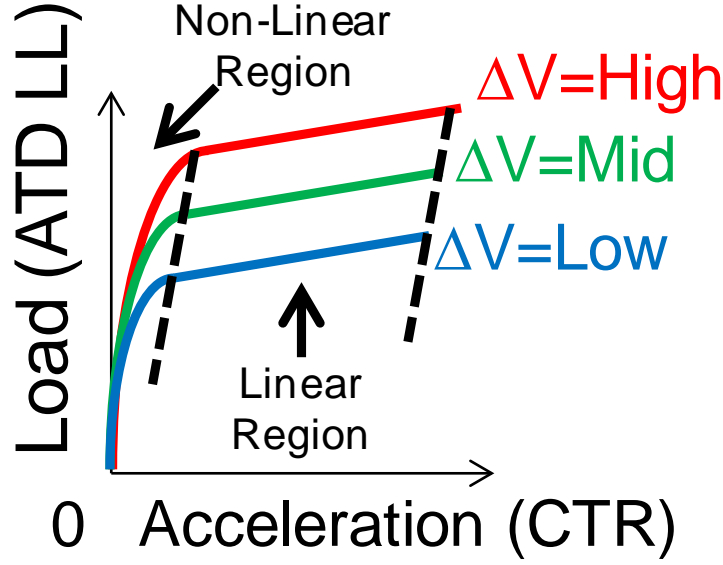


Fig. 24 Schematic of the amplitude-domain transfer relation between the CTR response and ATD lower-leg response

Considering the above, the amplitude-domain transfer relation was formularized. In the nonlinear region, the ATD lower-tibia load  $F_{LEG}$  is calculated as follows:

$$F_{ATD} = A \cdot a_{CTR}^2 + B \cdot a_{CTR}, \quad (1)$$

where  $a_{CTR}$  is the acceleration of the CTR crosshead, and A and B are the rate-dependent parameters in a loading condition. In the linear region,  $F_{LEG}$  is calculated as follows:

$$F_{ATD} = C \cdot a_{CTR} + F_{IP}, \quad (2)$$

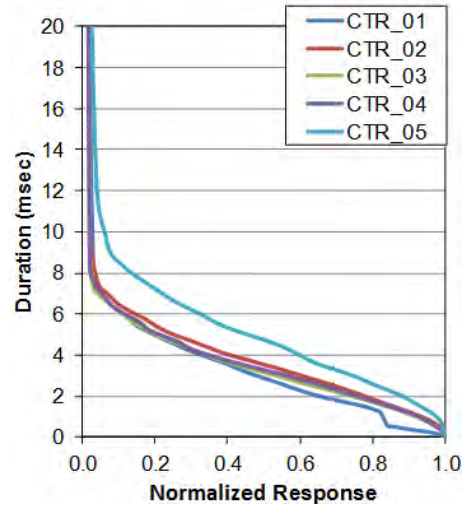
where  $F_{IP}$  is equal to  $F_{LEG}$  calculated in Eq.1 at the inflection point of the bilinear curve, and C is the averaged slope in the linear region among loading conditions. The Parameters A, B, and C were calculated for each loading condition (Table 6). Moreover, in the application of this transfer relation to other loading conditions, the parameters were calculated as the bilinear interpolation of the values in Table 6 according to the velocity change  $\Delta V$ .

Table 6 Parameters for Eqs. 1 and 2 in each loading condition

Loading Condition	Velocity Change, $\Delta V$ (m/s)	A	B	C
CTR_01 / ATD_01	3.52	-5.61E-06	7.29E-03	
CTR_03 / ATD_03	5.26	-2.22E-06	6.96E-03	3.20E-04
CTR_05 / ATD_05	6.62	-3.97E-06	1.10E-02	

Units: Load(kN), Acceleration( $m/s^2$ ), Time(msec)

Similar procedures were applied in the duration–domain comparison. Firstly, the responses of the CTR and ATD lower leg were normalized by their peak values. Secondly, as shown in Figs. 25 and 26, the relation between the duration and normalized response were analyzed according to the SAE J1727 injury-calculations guideline for decomposing the time domain signal into the duration domain signal.



**Fig. 25 Relation between the duration and normalized response of the CTR loading**

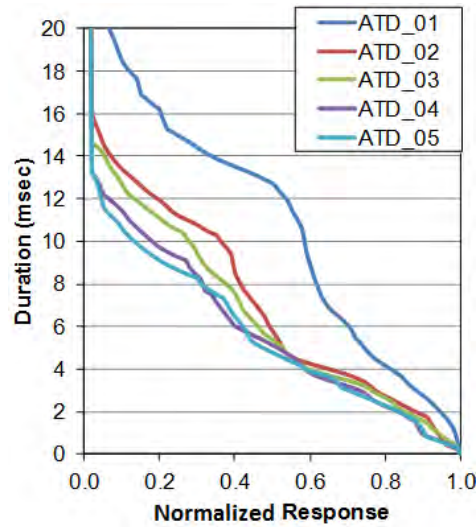


**Fig. 26 Relation between the duration and normalized response in the ATD lower-leg loading**

The responses of both test configurations were related in the duration domain as shown in Fig. 27. In this study, we focused on the 5-msec-pulse loading. Therefore, the maximum pulse duration is at most 8 msec in the CTR response, and we focus on the linear part of the duration–

domain transfer relation (Fig. 28). Thus, the ATD lower-tibia time duration  $T_{ATD}$  is calculated as follows:

$$T_{ATD} = D \cdot T_{CTR}, \quad (3)$$

where  $T_{CTR}$  is the CTR time duration. The parameter  $D$  was calculated as listed in Table 7 for each loading condition. In the application of this transfer relation to other loading conditions, the parameter was calculated as the linear interpolation of the value in Table 7 according to the  $\Delta V$ .

The ATD lower-leg response is predicted from the CTR response combining the amplitude–domain transfer and duration–domain transfer; a CFC600 filter is applied to ensure consistency with the appropriate lower-leg filter class from the CTR response.<sup>10</sup>

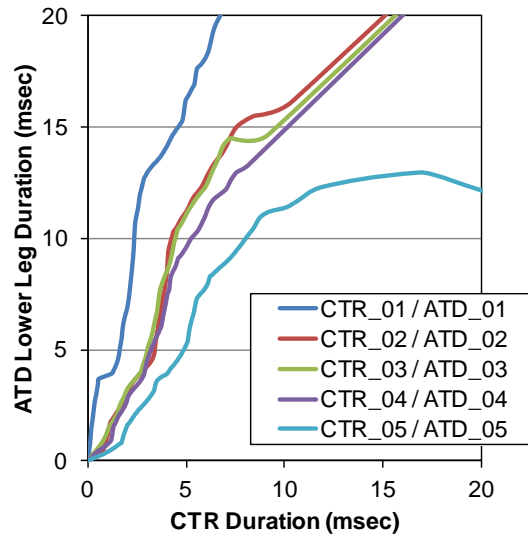


**Fig. 27 Relation of the pulse duration between the ATD lower-tibia response and CTR crosshead response in each loading condition**

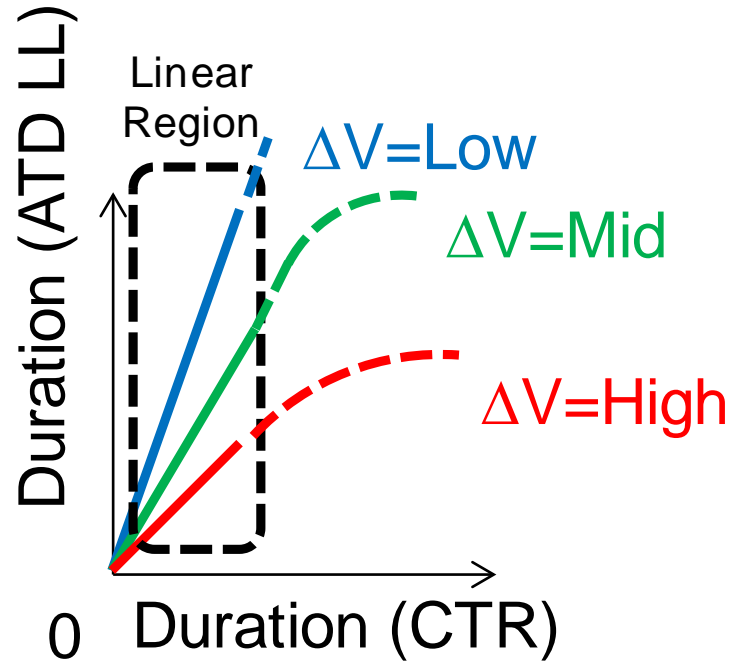


Fig. 28 Schematic of the duration–domain transfer relation between the CTR response and ATD lower-leg response

Table 7 Parameters for Eq. 3 in each loading condition

Loading Condition	Velocity Change, $\Delta V(\text{m/s})$	D
CTR_01 / ATD_01	3.52	1.84
CTR_03 / ATD_03	5.26	1.41
CTR_05 / ATD_05	6.62	1.10

Units: Load(kN), Acceleration( $\text{m/s}^2$ ), Time(msec)

### 3.2 Prediction of ATD Lower-Leg Response Based on the CTR Response

To confirm the validity, the transfer relation was applied to the CTR responses of 2 SKYDEX tests, which were not used in the development of the transfer relation. The predicted ATD responses are shown in Figs. 29 and 30 with the experimental ATD responses. To confirm the validity against other floor-mat material, the transfer relation was applied to the butyl-rubber floor mat using the FE model of the CTR and ATD lower leg. The FE-material model used for the butyl rubber in these FE models is listed in Table 8.<sup>9</sup>

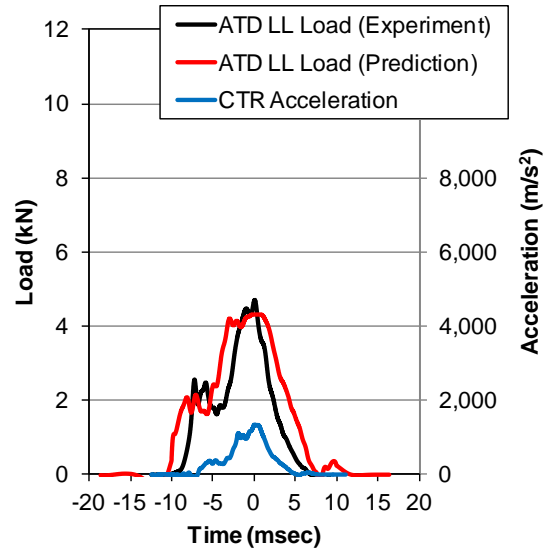


**Fig. 29** Comparison between the ATD lower-leg experimental response and predictive response from the CTR response, CTR\_02/ATD\_02 ( $\Delta V = 4.86$  m/s)

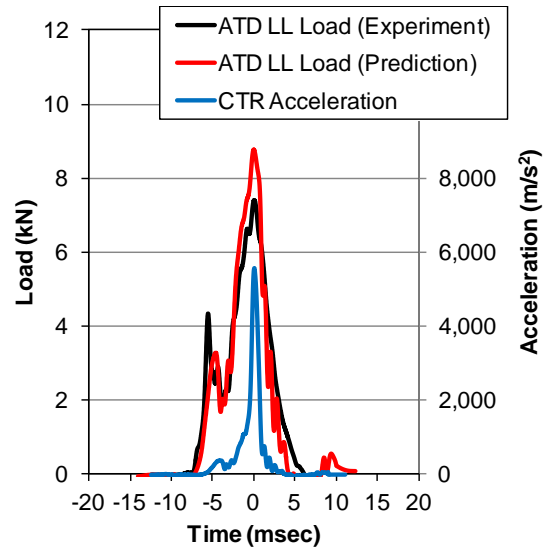


**Fig. 30** Comparison between the ATD lower-leg experimental response and predictive response from the CTR response, CTR\_04/ATD\_04 ( $\Delta V = 6.26$  m/s)

**Table 8 FE-material models for the butyl rubber**

Part	Material	Model Type in LS-DYNA	Model Description /Parameters
Floor Mat	Butyl Rubber	MAT_183 SIMPLIFIED_RUBBER_ WITH_DAMAGE	Incompressible Rubber Model with Strain-Rate Dependent Loading / Unloading Curves

The predicted ATD response from the CTR response in the FEA is shown in Fig. 31 with the ATD response in the FEA. The prediction errors of these comparisons are listed in Table 9.

The predicted ATD responses agree with those of the experiments including the plateau regions (second peaks), whereas the clues are not clear in the CTR responses. Especially, the peak loads are well predicted. However, the prediction overestimates the ATD lower-leg response in the large  $\Delta V$  loading. The treatment of the high acceleration in the CTR response needs to be revisited to increase the accuracy of the transfer relation.

In the application to the butyl-rubber floor mat, the prediction in the amplitude domain shows small errors. However, the prediction in the duration domain shows shorter duration response than the FEA result of the ATD lower leg. Thus, the impulses are underestimated. This may be because of the low reliability of the FE-material model in the unloading phase. Therefore, the experimental confirmation against other available material is anticipated.

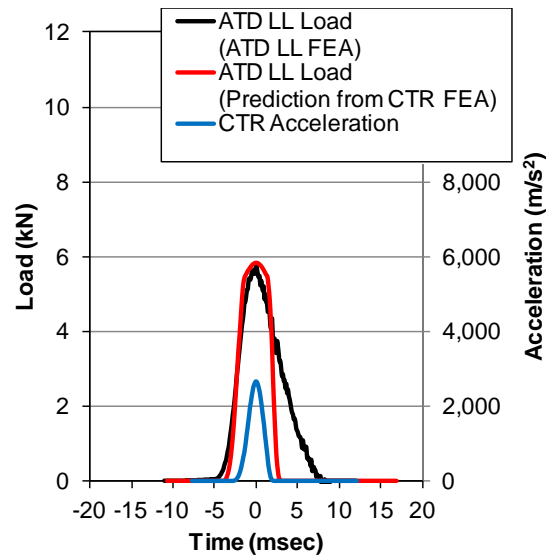


**Fig. 31 Example of the application of the transfer relation to the butyl-rubber floor mat in the FEA, CTR\_03/ATD\_03 ( $\Delta V = 5.26$  m/s)**

**Table 9** Errors in the ATD lower-leg response prediction from the CTR response

Floor mat material	Loading Condition	Velocity Change, $\Delta V$ (m/s)	Prediction Error in the Peak Load	Prediction Error in the Applied Impulse
SKYDEX	CTR_02 / ATD_02	4.86	-8%	37%
SKYDEX	CTR_04 / ATD_04	6.26	18%	-4%
Butyl Rubber	CTR_05 / ATD_05	5.26	2%	-24%

#### 4. Conclusions

In this study we developed the CTR to replace the ATD lower leg in the evaluation of the floor mat against underbody blast loading. Through the FEA, the CTR was designed to simulate the floor-mat loading status under the ATD lower leg during the loading event. Then, the transfer relation between the CTR response and ATD lower-leg response was clarified through the drop test with various loading conditions. Moreover, the validity and applicability of the transfer relation were confirmed with the experimental results of SKYDEX loading and FEA results of the butyl-rubber loading.

Through these processes, the CTR prototype was developed with the transfer relation for the prediction of ATD lower-leg response. For the improvement of the CTR, further loading tests with large  $\Delta V$  and other floor mats are recommended.

---

## 5. References

---

1. Dougherty AL, Mohrle CR, Galarneau MR, Woodruff SI, Dye JL, Quinn KH. Battlefield extremity injuries in Operation Iraqi Freedom. *Injury*. 2009;40(7):772–777.
2. Belmont PJ, Schoenfeld AJ, Goodman G. Epidemiology of combat wounds in Operation Iraqi Freedom and Operation Enduring Freedom: orthopaedic burden of disease. *J Surg Orthop Adv*. 2010;19(1):2–7.
3. Eskridge SL, Macera CA, Galarneau MR, Holbrook TL, Woodruff SI, MacGregor AJ, Morton DJ, Shaffer RA. Injuries from combat explosions in Iraq: injury type, location, and severity. *Injury*. 2012;43(10):1678–1682.
4. Test methodology for protection of vehicle occupants against anti-vehicular landmine effects. NATO; 2007. Report No.: TR-HFM-090.
5. Golan G, Asaf Z, Ran E, Aizik F. Occupant legs survivability: an assessment through the utilization of field blast test methodology. Paper presented at: MABS22. Proceedings of the 22nd International Symposium on Military Aspects of Blast and Shock; 2012 Nov 4–9; Bourges, France.
6. Dong L, Zhu F, Jin X, Suresh M, Jiang B, Sevagan G, Cai Y, Li G, Yang KH. Blast effect on the lower extremities and its mitigation: a computational study. *J Mech Behav Biomed Mater*. 2013;28:111–124.
7. Kargus RG. Laboratory evaluation of blast mitigating floor mats. Adelphi (MD): Army Research Laboratory (US); 2013 Jan. Report No.: (Sensitive Information Redacted Version).
8. Bailey AM, Panzer MB, Salzar RS. Development of a Hybrid-III to human leg transfer function for axial loading. Paper presented at: 10<sup>th</sup> Annual Injury Biomechanics Symposium. Proceedings of the Ohio State University Injury Biomechanics Symposium; 2014 May 18–20; Columbus (OH).
9. Sakamoto M. Experimental validation of the butyl-rubber finite element (FE) material model for the blast-mitigating floor mat. Adelphi (MD); Army Research Laboratory (US). 2015 Aug. Report No.: ARL-SR-0329.
10. Memorandum for Record. Updated accelerative loading criteria for crew injury. Army Research Laboratory (US); 2012 May.

---

## List of Symbols, Abbreviations, and Acronyms

---

ARL	US Army Research Laboratory
ATD	anthropomorphic test device
CSBES	Crew Survivability Blast Effects Simulator
CTR	Compression Test Rig
FE	finite element
FEA	Finite Element Analysis
IED	improvised explosive device
kN	kilonewton
LSTC	Livermore Software Technology Corporation
mm	millimeter
msec	millisecond
m/s	meters per second

1 DEFENSE TECH INFO CTR  
(PDF) ATTN DTIC OCA

2 US ARMY RSRCH LABORATORY  
(PDF) ATTN IMAL HRA MAIL & RECORDS MGMT  
ATTN RDRL CIO LL TECHL LIB

1 US ARMY RSRCH LAB  
(PDF) ATTN RDRL WMP F R KARGUS